Concentration dependences of heat conductivity coefficients of inert gases in narrow pores

Yu. K. Tovbin and V. N. Komarov*

State Research Center of the Russian Federation "L. Ya. Karpov Institute of Physical Chemistry", 10 ul. Vorontsovo Pole, 103064 Moscow, Russian Federation. Fax: +7 (095) 975 2450. E-mail: tovbin@cc.nifhi.ac.ru

Calculation of the transfer of molecules in porous systems requires self-consistent expressions describing the kinetic transfer coefficients for various concentrations and temperatures. The concentration dependences of heat conductivity and self-diffusion coefficients for fluids with different densities, ranging from rarefied gases to liquids, were considered in terms of a unified model. For monoatomic gases (argon), the model takes into account two energy transfer channels, namely, the vacancy mechanism and energy transfer through collisions of molecules. The former channel is characteristic of rarefied gases, while the latter is noted for condensed phases. The energy parameters of the model were determined on the basis of data on the heat conductivity coefficient in the bulk phase. The heat conductivity coefficient follows a linear temperature dependence for low density; in the medium and large density regions, these dependences follow a more complex pattern that changes depending on temperature. The influence of the interaction of atoms with the pore walls on the concentration dependences of the heat conductivity coefficients was investigated for different total amounts of the adsorbate. These coefficients depend appreciably on the distance to the pore wall and on the direction of heat transfer.

Key words: slit-like pores, adsorption, heat conductivity coefficient, self-diffusion coefficient, lattice-gas model, quasi-chemical approximation.

The transfer of molecules in porous solids plays[1—5] an important role in a large number of processes including catalysis, sorption, separation by membranes, *etc*. The pore size (H) in porous systems varies over a broad range.[6,7] According to M. M. Dubinin, pores are classified into micro-, meso-, and macropores.[6,7] In pores with 7—10 nm width, which can be defined as narrow,[8,9] the potential of the walls influences the aggregation state of the fluid formed by nonpolar gases, and, correspondingly, on the mechanism of its transport. All transport characteristics of the adsorbate in these narrow pores differ from those in the vapor or liquid phase. In the case of polar molecules, the effect of the wall potential is observed also in wider pores.

The most important dynamic characteristics of the adsorbate are self-diffusion and heat conductivity coefficients.[1—5] The theoretical calculation of these values for densities ranging from the gaseous to liquid state and for different temperatures causes certain difficulties even in the case of bulk phases. For porous systems, the situation is even more complicated. Some progress was made only in calculations of the dynamic characteristics of rarefied gases.[10] At present, self-diffusion coefficients of the adsorbate are calculated rather reliably by molecular dynamics[11—13] and measured experimentally[14,15] by NMR. No data on the heat conductivity coefficients for narrow pores are available. In some studies,[16—18] the dense heat flows between the walls of slit-like pores are simulated using molecular dynamics, while rarefied flows are described in terms of the kinetic theory.[19] However, concentration dependences of heat conductivity coefficients of dense gases and liquids in narrow pores of adsorbents have not yet been studied.

In porous systems with well-developed specific surface areas, low heat conductivity can bring about heat localization and, as a consequence, local overheated zones, which change local reaction rates. Thus, the change in the conditions of heat transfer between the opposite pore walls depending on the adsorbate density can markedly influence not only adsorption but also catalytic processes.

This work is the first theoretical study of the concentration dependences of the heat conductivity coefficient profiles of an adsorbate over a broad range of fillings of slit-like pores. We restrict ourselves to the case of a monoatomic fluid in order to eliminate the effect of the internal degrees of freedom on the heat conductivity coefficient. Only two energy transfer channels can exist in conventional dense fluids.[20—22] One channel is associated with the migration of particles through a specified plane 0,

Published in Russian in *Izvestiya Akademii Nauk. Seriya Khimicheskaya,* No. 11, pp. 1871—1880, November, 2002.

1066-5285/02/5111-2026 $27.00

as in a rarefied gas. The second channel is due to collisions between the molecules where the path of one molecule is blocked by another molecule located in the close vicinity on the different side of plane 0. Therefore, the lattice-gas molecular model provides the following structure of expressions for the heat conductivity coefficient:[23—25] $\kappa_{fg} = \kappa_{fg}^{(1)} + \kappa_{fg}^{(2)}$, where the superscript corresponds to the number of transfer channel, and the subscripts f and g specify the direction of transfer (see below). The additivity of contributions of the two channels follows directly from the existence of two alternatives for each molecule, it can either cross or not cross some specified plane 0.

In order to determine the contribution of the first channel to the κ_{fg} coefficients, one should know the local self-diffusion coefficients D_{fg}^*, which describe the transfer of "labeled" particles in the system at equilibrium due to the thermal motion of all particles.[21,26] To make the calculations more specific, one should determine the energy parameters of the adsorbate—adsorbate potential functions on the basis of the available experimental data on bulk concentration dependences of the heat conductivity coefficient.[27,28]

These problems can be solved using the lattice-gas model,[29,30] which takes into account the intrinsic volumes of atoms and the interactions between atoms in the quasi-chemical approximation. This model allows one to find self-consistent equilibrium characteristics of a vapor—liquid system and molecular transport coefficients in the bulk phase with the use of a unified set of energy parameters. It is applicable to fluid concentrations and temperatures varying over wide limits. The phase diagrams obtained using this model and specific features of the distribution of the shear viscosity factors are in good agreement with the data found by Monte Carlo and molecular dynamics calculations.[31—33]

Model

The lattice-gas model reflects the discrete distribution of molecules in space. The pore volume (V) is divided conventionally into a number of cells (sites) with dimensions of about the particle volume $v_0 = \lambda^3$ (λ is the lattice constant). Thus, $V = Nv_0$, where N is the number of sites in the system. Each site has z neighbors and can accommodate only one particle. It is assumed[34] that the particle can move inside the site. Thus, it is possible, on the one hand, to retain the whole formal apparatus of the lattice-gas model and, on the other hand, to use convenient approximations over the whole density range including the region of rarefied gases. If the center of gravity of a molecule is located inside the site, this site is regarded occupied and if the center of gravity is outside the site, it is regarded vacant. The occupancy state of a site with number f ($1 \le f \le N$) is specified by i: if the site is occupied by molecule A, i = A and if the site is vacant, i = v. The concentration $C = N_m/V$ is usually expressed as the number of molecules (N_m) in unit volume (*e.g.*, in 1 cm^3). In the lattice-gas model, the fluid concentration is described by the value $\theta = N_m/N_{den}$, which is the ratio of the number of particles in some volume to the number of close-packed particles ($N_{den} \equiv N$) in the same volume. Then $\theta = Cv_0$. The local density of particles i in site number f inside a pore will be designated by θ_f^i, and the local temperature will be denoted by T_f. The θ_f^A value characterizes the local fraction of occupied sites, while θ_f^v is the local fraction of vacant sites ($\theta_f^A + \theta_f^v = 1$, $\theta_f^A \equiv \theta_f$). The macroscopic density of the fluid θ in a distributed system of N cells is defined in terms of the local densities as

$$\theta = \sum_{f=1}^{N} \theta_f / N .$$

Each site f is characterized by a specific energy of interaction of molecules with the walls and, correspondingly, the Henry constant. In terms of this parameter, all sites of the lattice can be divided into groups with identical properties. The number of these groups will be designated by t. If the walls of a slit-like pore are homogeneous, all sites of the same layer are equivalent; therefore, the number of layer f coincides with the number of site located in it. For an even number of monolayers $t = H/2$, and for an odd number, $t = (H + 1)/2$. The local Henry constant $a_f = \beta F/F_0 \exp(\beta Q_f)$, where $\beta = (kT)^{-1}$ is the Boltzmann constant, F and F_0 are the sums of the states of particles inside the lattice system and outside this system (in the gas phase), respectively, Q_f is the energy of binding of a molecule in layer f with the pore walls and $Q_f = u(f) + u(H - f + 1)$ ($1 \le f \le t$); and the potential of interaction of the molecule with the pore wall $u(f) = \varepsilon_a/f^3$ corresponds to the "attraction" branch of the Mie(3—9) potential[35] (ε_a is the energy parameter of the pore wall potential).

The macroscopic density of fluid θ in a slit-like pore is described by the equation

$$\theta = \sum_{f=1}^{t} F_f \theta_f ,$$

where F_f is the fraction of sites pertaining to layer f;

$$\sum_{f=1}^{t} F_f = 1.$$

We will restrict ourselves to interactions of the closest neighboring molecules and designate the interaction energy between particles i and j (j = A or v) by ε_{ij}. Here, $\varepsilon_{AA} \equiv \varepsilon$, $\varepsilon_{iv} = 0$, *i.e.*, the interaction of particle i with a vacancy is null. The mutual distributions of molecules are described by pair distribution functions θ_{fg}^{ij}, which deter-

mine the probability that two particles *ij* occur in the neighboring sites *f* and *g*. Additionally, the following normalization relations hold: $\theta_{fg}^{AA} + \theta_{fg}^{Av} = \theta_f$ and $\theta_{fg}^{vA} + \theta_{fg}^{vv} = \theta_f^{v}$.

Equilibrium characteristics of the adsorbate

The pattern of pore filling depends appreciably on the wall potential. To calculate the heat conductivity coefficient for the adsorbate, one requires equilibrium characteristics, because the dynamic modes of disturbance of the thermal equilibrium have little influence on the equilibrium distribution of molecules. If only interactions between the adjacent neighbors are taken into account, the local isotherms that relate the local filling of the sites to the outer pressure *p* outside the pore are described by the expressions[30,36]

$$a_f p(1-\theta_f) = \theta_f \prod_{g \in z_f} (1 + x_{fg} t_{fg}), \qquad x_{fg} = \exp(-\beta\varepsilon) - 1, \qquad (1)$$

$$t_{fg} = 2\theta_g/(\delta_{fg} + b_{fg}), \qquad \delta_{fg} = 1 + x_{fg}(1 - \theta_f - \theta_g),$$

$$b_{fg} = (\delta_{fg}^2 + 4x_{fg}\theta_f\theta_g)^{0.5}.$$

The subscript *g* runs through a number of values corresponding to all the neighboring sites z_f around the central site in layer *f*; the function $t_{fg}^{AA} \equiv t_{fg} = \theta_{fg}^{AA}/\theta$ is the conditional probability that molecule A is located in site *g* near the "central" molecule A in site *f*. The equilibrium distribution of particles over different types of sites can be found by solving the set of equations (1) using an iteration procedure.

For calculating the heat conductivity coefficient, the specific heat $C_v(f)$ per particle is needed. This value is composed of kinetic and potential energy contributions $C_v(f) = C_v^{(1)}(f) + C_v^{(2)}(f)$.

$$C_v^{(1)}(f) = (3 + \sum_{g \in z_f - \Delta 1 f} t_{fg}^{AA}/2 + \Delta_{1f})k/2, \qquad (2)$$

$$C_v^{(2)}(f) = \mathrm{d}U_f/\mathrm{d}T, \; U_f = 0.5 \sum_{g \in z_f - \Delta 1 f} t_{fg}^{AA}\varepsilon_{fg} + \Delta_{1f}Q_1 + \Delta_{2f}Q_2,$$

where U_f is the potential energy of the molecule located in site *f*. The U_f value consists of contributions of intermolecular interactions (the first sum) and the adsorbate—adsorbent interactions (the second two summands for the first two near-surface layers; for other layers, the contribution of the wall potential is neglected). The Δ_{ij} value is the Kronecker symbol ($\Delta_{ii} = 1$ for $i = j$ and $\Delta_{ij} = 0$ for $i \neq j$); $C_v^{(2)}(f)$ is the configurational contribution to the specific heat caused by intermolecular interactions. In calculation of the derivative with respect to temperature, the overall adsorbate density in the pore is taken to be constant. The expressions for $C_v^{(2)}$ in a homogeneous system were considered previously.[37] The contributions of the kinetic energy for the translational motion of particles in the gas bulk ($C_v^{(1)} = 3k/2$) and oscillations for the liquid phase ($C_v^{(1)} = zkt_{AA}/2$) are different.[23] In the case of a dense phase, where $t_{AA} \approx 1$, we have[20] $C_v^{(1)} = 3k$. If $z > 6$, then, taking into account the projection of the particle motion onto directions of different axes, we obtain the same final result for the dense phase of the fluid, namely, $C_v^{(1)} = 3k$. Relation (2) presents this contribution for an inhomogeneous fluid.

The first channel of heat conduction

Two energy transfer channels exist in dense fluids. One is associated with the same particle movement as in a rarefied phase, while the other is determined by collisions of particles. The thermal motion of molecules is accompanied by transfer of their own energy in different directions. The resultant flow of such molecular motion along some direction can be expressed in terms of the self-diffusion coefficient. However, narrow-pore systems are highly heterogeneous, and the thermal motion in them is essentially anisotropic due to the influence of the pore wall potential. As a consequence, the contribution of the first heat conduction channel to the corresponding coefficient κ_{fg} becomes anisotropic. The local coefficients of heat conductivity along the first channel can be calculated using the equation[24,25]

$$\kappa_{fg}^{(1)} = C_v(f)\theta_f D^*_{fg}. \qquad (3)$$

The local self-diffusion coefficient in heterogeneous media corresponding to the distribution of "labeled" molecules between neighboring sites at equilibrium is described by the following equation:[30,38,39]

$$D^*_{fg} = z^*_{fg}\lambda^2 W_{fg}/\theta_f, \qquad (4)$$

where z^*_{fg} is the number of possible jumps of the particle located in site *f* into the neighboring sites of layer *g*, and W_{fg} is the rate of molecule jumping from site *f* into a vacant site *g*. For the simplest case of jumping to the nearest neighboring sites, this rate can be described by the formula[30,38,39]

$$W_{fg} = k_{fg}V_{fg}, \qquad (5)$$

where

$$k_{fg} = F^* \exp(-\beta E_{fg})/(\beta h F),$$

$$V_{fg} = \theta_{fg}^{Av} T_{fg}, \qquad T_{fg} = \prod_{\xi \in z_f - 1} S^{A}_{f\xi} \prod_{\zeta \in z_g - 1} S^{v}_{g\zeta}.$$

Here, k_{fg} is the rate constant for particle jumping from site *f* to the nearest vacant site *g* in an unfilled lattice, F^* and *F* are the statistical sums of the particle states in the transition and ground states, respectively, *h* is Planck´s

constant, and E_{fg} is the activation energy of jumping. In the case of sites located far from the pore walls, $E_{fg} = 0$, while for those located near the walls possessing an adsorption potential, $E_{fg} \neq 0$. The rate constants for jumps for various sites comply with the following condition: as the energy well becomes deeper, the probabilty for a particle to leave it decreases. The relationship between the hopping constants and the local Henry constants is represented by expressions $a_f k_{fg}^{Av} = a_g k_{gf}^{Av}$. Here, we take into account that $a_f = a_f^0 \exp(\beta Q_f)$.

The concentration dependence of the migration rate in relation (5) is inherent in the term V_{fg}, which, in turn, consists of the factors θ_{fg}^{Av} and T_{fg}. The θ_{fg}^{Av} value describes the probability that a vacant neighboring site g is located near the particle A in site f, and T_{fg} takes into account the effect of interactions between the molecules arranged around the central Av pair in sites fg on the energy of the activated complex. The factor $S_{f\xi}^{A} = 1 + t_{f\xi}x^*$ present in the expression for T_{fg} refers to $z - 1$ adjacent neighbors ξ of molecule A in site f that occur in the ground state (site g is excluded from neighbors of A). Similarly, the term $S_{g\zeta}^{v} = 1 + t_{g\zeta}^{vA}y^*$ refers to the $z - 1$ neighbor of vacant site g. Here, $x^* = \exp[\beta(\varepsilon^* - \varepsilon)] - 1$, $y^* = \exp(\beta\varepsilon^*) - 1$, where ε^* is an energy parameter of interaction of a particle occurring in the transition state with a neighboring ground-state particle. In the absence of lateral interactions, formula (5) acquires the form $W_{fg} = k_{fg}\theta_f(1 - \theta_g)$. At a distance from the pore walls, the F/F^* ratio reduces to the statistical sum of the translational degree of freedom in the direction of particle movement, this sum being equal to $(2\pi m\beta^{-1})^{1/2}\lambda/h$, where m is the mass of the molecule. Then the rate constant for jumping in the bulk phase $k_{fg} = w/4\lambda$, where $w = (8/\pi m\beta)^{1/2}$ is the velocity of the thermal motion of the molecule in the gas phase.[20]

As a rule, local self-diffusion coefficients (4) are replaced by an averaged characteristic of the thermal motion of "labeled" (*e.g.*, isotopic) molecules along the pore axis. This characteristic is the self-diffusion coefficient described by the relation[30,38,39]

$$D^* = \lambda^2 \sum_{f=1}^{t} F_f \sum_{g=1}^{t} z_{fg} W_{fg}/\theta_f \frac{d\theta_f^*}{d\theta^*}, \qquad (6)$$

where $d\theta_f^*/d\theta^* = d\theta_f/d\theta$. Expression (6) takes into account all the possible jumps of a migrating molecule to the neighboring sites of various types. The averaging was done over the contributions to the overall flow made by both the sites to which the molecule migrates (type g site) and the sites from which it migrates (type f site).[33,40]

The second channel of heat conduction

Now we will calculate the contribution of the energy transfer through particle collision in a dense fluid to the heat conductivity coefficient; for this purpose, we consider an energy flux transferred *via* oscillations of neighboring molecules.[23—25] Each oscillation along the flux direction ensures the transfer of a particular amount of energy due to collisions of particles located in adjacent planes f and g at distance λ. The transfer is performed $2\nu_{fg}$ times per second by each of the θ_f particles situated near the plane separating the neighboring sites f and g through which the energy flux is calculated (the location of a molecule rather than vacancy in site g adjacent to site f is taken into account by the function t_{fg}^{AA}). The characteristic time of oscillational relaxation is shorter than the characteristic time of the local hops of molecules, which change the function t_{fg}^{AA}. Upon collision, each particle transfers the energy $C_v(f)T_f$, where $C_v(f)$ is the specific heat per molecule introduced above. The energy flux can be represented as $J = 2z_{fg}^*\nu_{fg}\lambda[S(x = -\lambda/2) - S(x = \lambda/2)]/6$, where $S = \theta_f C_v(f) T_f$. The proportionality coefficient obtained on expansion of the J value over the temperature gradient in the neighboring sites f and g corresponds to the local heat conductivity coefficient. This expansion gives the expression

$$\kappa_{fg}^{(2)} = z_{fg}^*\theta_{fg}^{AA}C_v(f)\lambda^2\nu_{fg}/3. \qquad (7)$$

To simplify the calculation of the harmonic oscillation frequency of the central molecule ν_{fg} in site f, the calculations were done using the (1) Lennard—Jones (6—12) potential, (2) averaged $\mu(f)$ value for the reduced mass of the adsorbate molecule in site f, and (3) averaged U^*_f value of the potential binding energy of the central molecule in site f:

$$\nu_{fg} = [48U^*(f)/\mu(f)]^{0.5}/2\pi r_{fg}^{min},$$

$$U^*_f = (0.5 \sum_{g \in z_f - 1 - \Delta_{1f}} t_{fg}^{AA} + 1)\varepsilon_{fg} + \Delta_{1f}Q_1 + \Delta_{2f}Q_2. \qquad (8)$$

In the case of a heterogeneous system with variable density, the μ value is calculated for each site f using the relation

$$\mu(f)^{-1} = m^{-1}(\sum_{g \in z_f - \Delta_{1f}} t_{fg}^{AA} + 1) + \Delta_{1f}m_s^{-1},$$

where m is the mass of the adsorbate molecule and m_s is the mass of the atom (or atoms) of the solid (adsorbent), which has to be taken into account if the adsorbate is positioned in the near-surface layer. The expression for $\mu(f)$ allows for all particles surrounding the central molecule in site f. If the adsorbate is located in the first near-surface layer, one of its neighbors is always an atom (or atoms) of the solid (depending on the type of bonds between the molecule with the adsorbent), and the contribution of other neighboring molecules g is averaged over the other $z_f - 1$ sites. Note that formula (8) for U^*_f differs from formula (2) for the average energy of molecule U_f.

This is due to the necessity of bringing expression (8) for ν_{fg} in correspondence with the frequency of an isolated pair of molecules (dimer) in a rarefied gas. As the density decreases, U_f tends to zero and U^*_f tends to ε. This does not contradict expression (2), because the number of dimers itself also tends to zero following a decrease in the density of molecules. The difference between U_f and U^*_f is due to the different functional dependences describing the variation of the average potential energy and the oscillation frequency of molecules *vs.* the fluid density.

The anisotropic pattern of distribution of neighboring molecules θ_{fg}^{AA} causes anisotropy of the contribution of the second channel to the energy flux. Since the local self-diffusion coefficients are also anisotropic, the total heat conductivity coefficient $\kappa_{fg} = \kappa_{fg}^{(1)} + \kappa_{fg}^{(2)}$ is also anisotropic. The κ_{fg} values corresponding to different positions of molecules in a pore and different directions of their migration are dictated by the molecular properties of the adsorbent—adsorbate system (the particle masses and interaction potentials). When the fluid concentration is low, κ_{fg} is described by a linear concentration dependence, while for high concentrations, the θ exponent may reach 3—4.

Bulk phase and conditions of analysis of slit-like pores

If the distance between the walls of a slit-like pore is much greater than the radius of the adsorbate—adsorbent potential, the contribution of the adsorption potential of the walls can be neglected. Thus Eqs. (1)—(8) are simplified and become suitable for describing the equilibrium and dynamic characteristics of a homogeneous bulk phase (gas or liquid). This fact was used to determine the parameters for the lateral interaction of the adsorbate in the model considered. The interaction potential ε between the argon atoms was determined from the equation of state for a bulk phase (using the dependence of the compressibility factor $Z = p/(nkT)$ on the pressure p, here n is the number of molecules in 1 m^3), while the ε* value was found using the pressure dependence of the heat conductivity coefficient. The experimental data were described[27,28] in terms of a Lennard—Jones type effective potential. The depth of the potential function well $\varepsilon = \varepsilon_{ef}$ depends[41,42] on the density and on the temperature

$$\varepsilon_{ef} = \varepsilon_0 (1 - d_e\theta)(1 + uT), \qquad (9)$$

where ε_0 is the well depth for the nonmodified Lennard—Jones potential (238 cal mol^{-1}) corresponding to the well depth for an isolated argon dimer. The ε_0 value is known; it can be found by analyzing the second virial coefficients.[20] The second multiplier in function (9) takes into account the contributions of ternary interactions between the nearest neighboring molecules,[30] which modify the pair interaction potential: d_e is the ratio of the contribution of ternary interactions to the contribution of the binary interactions of the nearest neighbors. The u parameter describes the temperature dependence of ε_{ef}.

The compressibility factor in the bulk phase was calculated using a modified lattice-gas model[41,42] taking into account the pair interactions in four coordination spheres, the ternary interactions in the first coordination sphere, and the change in the lattice parameter upon an increase in the fluid density. Comparison of experimental data on

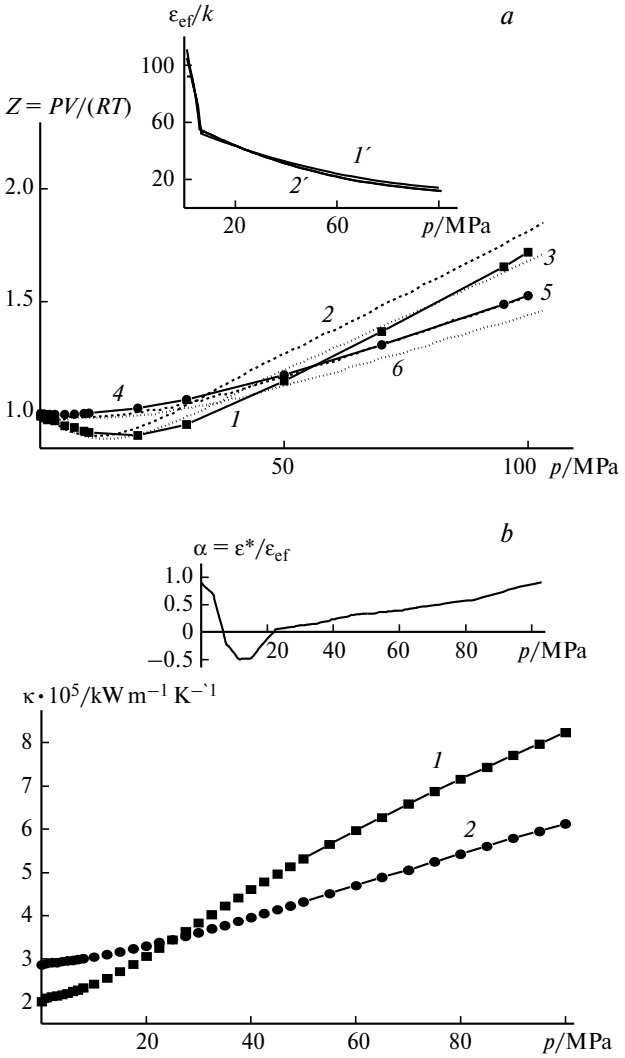

Fig. 1. Comparison of the experimental data[27,28] and theoretical curves for the dependence of compressibility factor (*a*) and heat conductivity coefficient (*b*) on the argon pressure in the bulk phase at 273 (*1—3*) and 400 K (*4—6*). (*a*) The dashed lines *2* and *5* correspond to calculations in terms of the rigid-lattice model, the dotted lines *3* and *6* represent the calculations by the compressible-lattice model. The inset shows the dependences of ε_{ef}/k on the argon pressure at 273 (*1′*) and 400 K (*2′*). (*b*) Calculation by the compressible-lattice model. The inset shows the dependences of $\alpha = \varepsilon^*/\varepsilon_{ef}$ on the argon pressure at $T = 273$ K.

the dependence of the compressibility factor on the fluid density for 273 and 400 K (Fig. 1, *a*) and the results of calculations carried out for rigid and compressible lattices over the pressure range from rarefied gas to a thousand atmospheres shows satisfactory agreement.

The ε_{ef} value is an energy characteristic of a lattice system. This value is found by averaging the initial Lennard—Jones atom—atom potential over the unit cell volume;[43] therefore, ε_{ef} depends on the fluid concentration and the system temperature (see Fig. 1). The decrease in the ε_{ef} values with respect to the ε_0 value and the negative temperature parameter u are consistent with the results obtained previously.[43] The resulting ε_{ef} values were used to describe heat conductivity coefficients in the same range of argon pressures and at the same temperatures.

The concentration dependences of the heat conductivity coefficient were analyzed using previously described modifications of the interaction potential between argon atoms (as well as the compressibility factor). Figure 1, *b*, shows comparison of the experimental data[27,28] with the theoretical curves derived in terms of the model with allowance for the lattice compressibility. The concentration dependence of the function of the parameter $\alpha = \varepsilon^*/\varepsilon_{ef}$ is shown in the inset for 273 K (a similar pattern is found for the curve for α at 400 K). The complicated pattern of the $\alpha(p)$ curve at low pressures is partially due to the low parameter sensitivity of the model in the rarefied gas region.

The results show that the lattice model provides a satisfactory description of the bulk properties of inert gases (argon) at pressures of <1000 atm. It should be noted that the problem of describing self-consistent equilibrium and dynamic characteristics of molecules over broad ranges of variation of the bulk phase density and temperature has not yet been finally solved;[20,21,27,28] however, its discussion is beyond the scope of the given study.

When simulating porous systems, we restricted ourselves to considering the adsorption of argon atoms in slit-like pores of graphite. The binding energy between the argon atoms and the graphite surface (Q_1) was described using the following relations:[44,45] $Q_1 = 9.24\varepsilon_0$, $Q_2 = Q_1/8$ (in conformity with the Mie(3—9) potential), and other $Q_f = 0$. Although an increase in the fluid density is known[46] to decrease the lattice parameter λ by ~10%, in this study, we used a coarser model of the adsorbate—adsorbate interaction potential for calculations. In these calculations, we assumed that the lattice parameter does not depend on the degree of pore filling and took into account only contributions from the interactions between the adjacent neighbors. Equations (1)—(8) were applied to a rigid lattice with the fixed value $\lambda = r_{min} = 2^{1/6}\sigma$, where σ is the Lennard—Jones potential parameter corresponding to the size of particle as a hard sphere. In this case, changes in the harmonic frequencies of atom oscillations are due, according to expression (9), only to the effect of the close surrounding on the U^*_f energy.

All calculations of the concentration dependences refer to a temperature of 273 K, which an above-critical temperature for Ar. We considered a cubic lattice ($z = 6$), which ensures the best description for the bulk critical parameters.[20,29,30,47,48] General analysis of the concentration dependences of the heat conductivity coefficient in narrow slit-like pores was performed using the following values: pore width $H = 10$ monolayers; binding energy of the adsorbate with the pore surface $Q = 9.24\varepsilon_0$; relative activation energy for particle jumping along the surface of the pore wall $\alpha_{11} = E_{11}/Q_1 = 1/3$ (this means that the particle movement along the surface has a low energy barrier). In order to counterbalance to some extent the drawbacks of the rough approximation inherent in the interaction potential, we used three sets of energy parameters instead of one set.

Variant	ε_0/cal mol^{-1}	d_ε	α
1	120	0	0.5
2	153.5	0.477	$-0.25 + 1.05\theta$
3	238	0	0.5

Variant *1* includes a dimensionless parameter α, often used in kinetic models.[30,39] According to variant *2*, which reflects the properties of the bulk phase outside the rarefied gas region, ε_{ef} is described by formula (9). The data for variant *3* correspond to traditional views on the properties of gaseous argon.[20]

This selection of the model parameters allows one to elucidate the influence of the energy characteristics of the intermolecular interactions, the contribution of the near-surface region to the overall effect of energy transfer, and the relationships between the energy transfer channels on the concentration dependences of the heat conductivity coefficients.

Results and Discussion

Let us first consider the concentration dependences of the system molecular characteristics that appear in the expression for heat conductivity coefficient.

Figure 2, *a* presents the dependences* of the layer-by-layer coverage θ_f of a 10-monolayer wide slit-like pore on

* From here on, the curves for local characteristics are designated by two digits. The digit before the hyphen means the number of the monolayer to which the parameter of adsorbed molecules refers (the monolayer coverage, heat capacity, vibration frequency or heat conductivity). The digit after the hyphen designates the number of the set of potentials used in calculations. For example, designation *1-2* for the curve in Fig. 2, *a* implies θ_1 for the calculation according to the second variant and *3-1*, *4-1*, and *5-1* are the local coverages of layers *3*, *4*, and *5* calculated in terms of the first set of potentials.

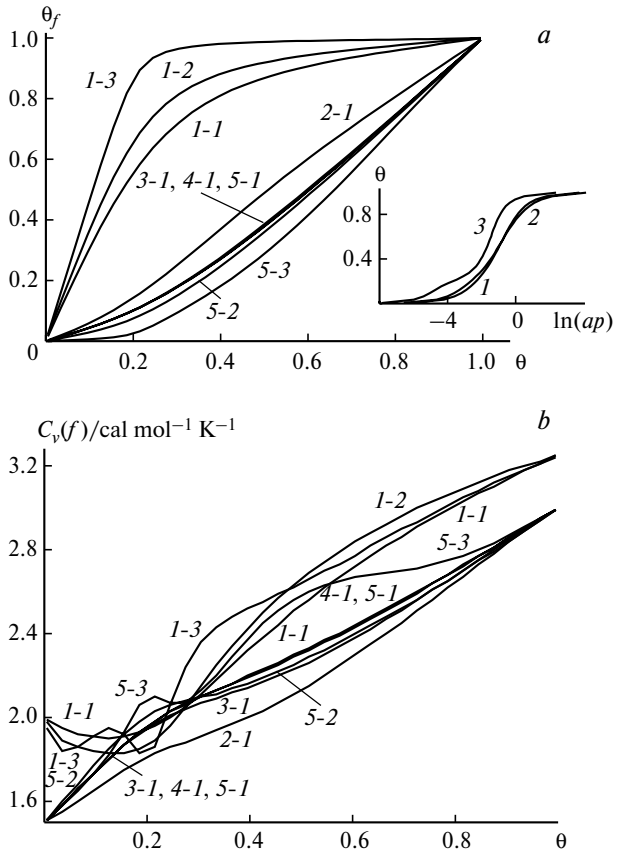

Fig. 2. (*a*) Profiles of argon concentration θ_f in a slit-like pore of graphite with a width of $H = 10$ monolayers. Here and below, the first digit in a curve corresponds to the monolayer number f (counting off from the pore wall). The inset shows the adsorption isotherms in the dimensionless coordinates θ—ln(ap). (*b*) Dependences of the specific heats $C_v(f)$ of layers *1*—*5* on the total degree of pore filling.

the degree of the overall filling of the pore θ. Comparison of three adsorption isotherms for different intermolecular interaction potentials (see the inset in Fig. 1, *a*) shows that isotherms *1* and *2* are rather close to each other. Isotherm *3*, corresponding to a stronger intermolecular interaction, shows that at higher pressures, the pores are filled more rapidly. For the sake of simplicity, the family of the curves shown in Fig. 2 corresponds only to the first variant of the potential, while for the second and third potential types, characteristics corresponding to the surface and central monolayers are presented. For any potential type, the first (surface) monolayer is the first to be filled (curves *1-1*, *1-2*, and *1-3*), the modes of filling of the central (the fourth and fifth) layers are virtually identical (curves *4-1* and *5-1*), and the effect of the wall can here be neglected. The filling of the third monolayer (curve *3-1*) differs little from that of the central layers. Although curve *2-1* for the second monolayer occupies an intermediate position, it is displaced toward other curves for the inner layers. (This pattern of the curve arrangement is retained for other characteristics) As the adsorptive pressure increases, the adsorbate density changes from values typical of the gas phase to densities corresponding to the liquid phase.

The curves for the variation of the specific heat of separate monolayers $C_v(f)$ *vs.* coverage of the first monolayer differ sharply from the curves for the inner layers, which are rather close to each other; the curves for layers *3*, *4*, and *5* are almost indistinguishable (see Fig. 2, *b*). As the pore coverage increases, the heat capacity of the fluid, as can be seen in Fig. 2, *a*, changes from values typical of gases to those corresponding to the liquid phase. In the two first near-surface layers. an additional contribution is made by the interaction potential with the surface. In the case of high densities, the greatest contribution to $C_v(f)$ is due to the kinetic component $C_v^{(1)}(f)$, while the potential energy component $C_v^{(2)}(f)$ does not exceed 10%. For low coverages, the $C_v^{(2)}(f)$ and $C_v^{(1)}(f)$ contributions are comparable and have different signs. Therefore, the resultant curves at low densities show a nonmonotonic pattern. This effect, inherent in inhomogeneous adsorption systems, is related to particle redistribution between the first and second monolayers, whereas for homogeneous systems,[37] the $C_v^{(2)}(f)$ contribution is markedly smaller than $C_v^{(1)}(f)$.

Figure 3 shows the concentration dependences for the local self-diffusion coefficients D^*_{fg} (curves *2*—*7*) and for the average self-diffusion coefficient D^* for particle movement along the pore axis (curve *1*). The curves were plotted in the dimensionless form with normalization to the corresponding self-diffusion coefficient for the bulk gas phase (for $\theta = 0$ and $Q_1 = 0$). The local coefficients decrease with an increase in the pore coverage, because free pore volume decreases. The movement of molecules in the (near-surface) layer is changed most appreciably

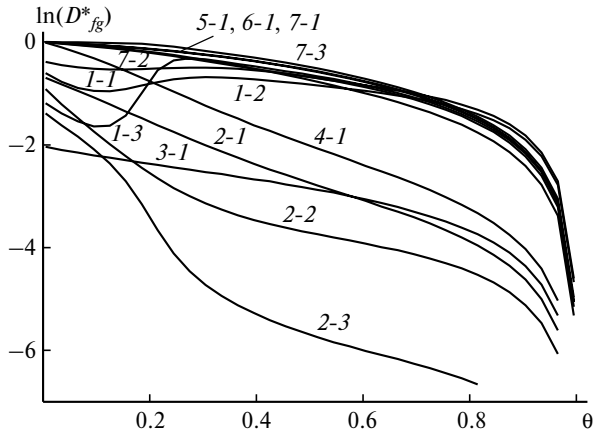

Fig. 3. Self-diffusion coefficients D^*_{fg} of argon in slit-like pores of graphite with a width of $H = 10$ monolayers *vs.* degree of pore filling. Curves *1* are the logarithms of the average D^*, the curve numbers correspond to the following pairs of neighboring sites in the layers: fg = 11 (*2*), 12 (*3*), 21 (*4*), 22 (*5*), 33 (*6*), 55 (*7*).

(curves *2-1*, *2-2*, and *2-3*). During filling of this layer, at $\theta < 0.2$, when a monolayer film has mainly formed (see Fig. 2, *a*), the self-diffusion coefficient D^*_{11} decreases. Further decrease in D^*_{11} is related to film compaction. For migrating from the first layer to the second, a molecule has to overcome the binding energy, equal to Q_1, therefore, curve *3-1*, which corresponds to D^*_{12}, is located below all other curves at low densities. The reverse migration of a molecule from the second to the first layer is characterized by the D^*_{21} coefficient and the corresponding curve *4-1* repeats the pattern of curve *2-1*. The decrease in this value is also associated with filling of the first layer. When the degree of pore filling is low, the movement of a molecule in the second layer (curve *5-1*) occurs virtually in the same way as in the pore center (curves *7-1*, *7-2*, and *7-3*). The decrease in D^*_{22} becomes noticeable when $\theta > 0.2$, after the surface monolayer has been filled. The average diffusion coefficient (curves *1-1*, *1-2*, and *1-3*) follows a nonmonotonic dependence on θ. This value includes the contributions caused by filling of individual layers; therefore, initially, it is close to D^*_{11}, at low coverages, it resembles the curve for the second layer, and at high coverages, it approaches the curve describing the layers in the central section of the pore. The ratio of the D^* values found for $\theta = 0$ and near the maximum of curve *1* depends on the activation energy of the surface migration of E_{11}, in particular, the smaller the E_{11}, the greater D^* ($\theta = 0$).

Analysis of the concentration dependences of the oscillation frequencies of Ar atoms in different layers of fluid f (Fig. 4, *a*) and similar dependences of the reciprocal reduced mass values μ^{-1} (Fig. 4, *b*) indicates that the values increase monotonically with an increase in the total adsorbate content in the pore and that the patterns of variation are similar. It can be clearly seen that the adsorption potential substantially affects the first monolayer and has a weaker influence on the second monolayer. The dependences for other monolayers are close to each other.

Figure 5 presents the concentration dependences of the overall heat conductivity coefficient along two channels for different pairs of neighboring sites. As in Fig. 3, the curves are given in the dimensionless form, normalization was done to the bulk heat conductivity coefficient for a rarefied gas. Comparison of the curves corresponding to contributions of the first and second channels (Fig. 5, *b*, *c*) shows that the first channel predominates at low coverages but, as the pore is filled, the contribution of this channel substantially decreases, and for medium or high coverages, the overall coefficient is determined by the second channel of heat conduction. The region of high mobility of adsorbate atoms in the near-surface layer can be clearly seen in Fig. 5, *b*: curves *1-1*, *1-2*, and *1-3* pass through a maximum as the first layer is filled (here, we consider a structured surface wall; however, the activation energy of

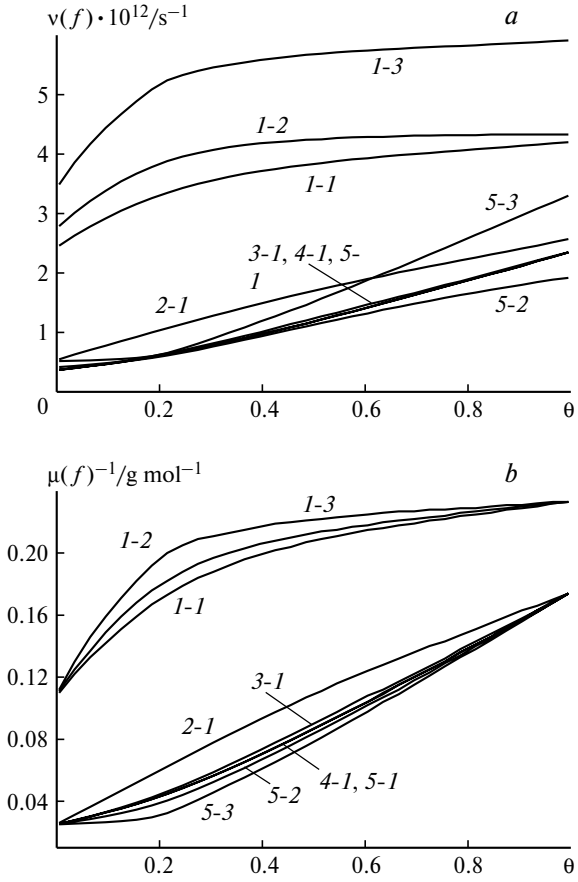

Fig. 4. Concentration dependences of the oscillation frequencies of argon atoms (*a*) and the reciprocal reduced mass values (*b*) in the argon—carbon pore system comprising $H = 10$ monolayers.

surface migration is relatively low). The relatively small changes in $\kappa_{12}^{(1)}$ and $\kappa_{21}^{(1)}$ (curves *2-1* and *3-1*, see Fig. 5, *b*) are due to high energy needed for abstraction of a molecule for migration from the first layer to the second one and to the predominant filling of the first layer, which prevents transition of the fluid from the second layer to the first one. Curves *4-1*, *5-1*, and *6-1* vary in a similar way: in this case, the effect of the wall is insignificant and, as the pore bulk is being filled, the contribution of the first heat conduction channel to the total energy remains insignificant. The pattern of the curves corresponding to the second channel (see Fig. 5, *c*) indicates that as the layer moves away from the wall, the contribution of the corresponding local heat conductivity coefficients progressively becomes smaller, although the coefficients themselves increase as the pore is filled by the adsorbate. Generally, Fig. 5 illustrates the important role of the adsorption potential contribution. The overall heat conductivity coefficient exhibits the same trends. It should be noted that the fourfold change in the heat conductivity coefficient in the bulk phase following a pressure increase from 1 to 1000 atm is in line with the 4—7-fold variation of κ_{fg} for the central

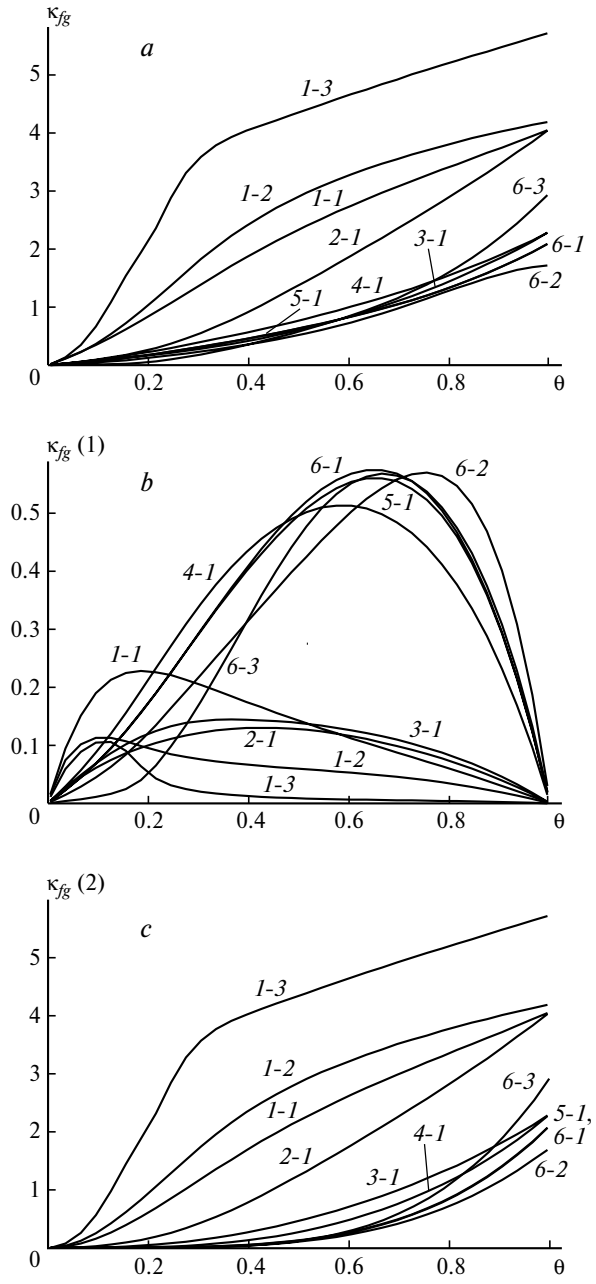

Fig. 5. Concentration dependences of the total heat conductivity coefficient (*a*), contribution of the first (*b*) and second (*c*) channels in a slit-like pore with a width of $H = 10$ monolayers. The curves correspond to the local κ_{fg} values for the following pairs of neighboring sites in the layers: fg = 11 (*1*), 12 (*2*), 21 (*3*), 22 (*4*), 33 (*5*), 55 (*6*).

part of a slit-like pore (curves *6-1*, *6-2*, and *6-3*, differing in the adsorbate—adsorbate interaction potential) after formation of two monolayers (for $\theta \approx 0.4$).

* * *

This study is concerned with the model of calculation of heat conductivity coefficients for spherically shaped adsorbate particles in narrow pores with 7—10-nm width. The upper limit of 7—10 nm implies 25—30 monolayers over which the surface potential affects the conditions of capillary condensation. The diameter of the adsorbate molecule determines the monolayer size but has no influence on the scope of applicability of the model. The model limitations are due to the fact that the inner degrees of freedom, inherent in polyatomic molecules, are not taken into account.

The procedure of calculation of the concentration characteristics of transfer parameters for dense fluids in narrow pores implies that a local equilibrium velocity distribution of molecules is achieved. This approximation is justified only in the case of relatively high adsorbate densities; it is applicable to liquid-like systems in the range of $(0.01—0.03) < \theta < 1.0$. When $\theta < 0.01$, this model requires correction. An important role of the pore width is indicated by the following estimate. According to the elementary kinetic theory of gases,[24] the frequency of collisions of Ar atoms with the walls in <7.0-nm pores is ~2 orders of magnitude greater than the frequency of their collisions with one another in the gas phase (at $T = 300$ K and a pressure of 1 atm). This means that the collision frequency of molecules in narrow pores, even in a rarefied system, is two orders of magnitude higher than in the gas bulk. Correspondingly, in narrow pores, the equilibrium is established faster as a result of collisions of molecules both with the pore wall and with one another. Therefore, this model provides reasonable estimates for the mass and energy transfer coefficients, although it does not take into account the dynamic effects associated with the variance of the velocity distribution of molecules.

The calculations show that dynamic characteristics of the adsorbate depend appreciably on the anisotropic distribution of molecules over the cross-section of a slit-like pore. The change in the heat conductivity and self-diffusion coefficients with respect to those in a homogeneous gas or liquid bulk phase is especially pronounced near the pore walls. In the pore center, these values depend slightly on the wall potential and are determined by the total adsorbate concentration. It follows from the obtained results that the traditional assumption of invariability of heat conductivity coefficients[2] is not true in the general case. When analyzing experimental data, one should take into account the rather pronounced concentration dependence of the dynamic characteristics of the adsorbate in narrow pores caused by the influence of the molecular interaction potentials with the pore walls and with one another.

This work was supported by the Russian Foundation for Basic Research (Project No. 00-03-32153).

References

1. D. P. Timofeev, *Kinetika adsorbtsii* [*Adsorption Kinetics*], Izd. Akad. Nauk SSSR, Moscow, 1962, 252 pp. (in Russian).

2. V. V. Rachinskii, *Vvedenie v obshchuyu teoriyu dinamiki sorbtsii i khromatografii* [*Introduction to the General Theory of Sorption and Chromatography*], Nauka, Moscow, 1964, 134 pp. (in Russian).
3. C. N. Satterfield, *Mass Transfer in Heterogeneous Catalysis*, MIT Press, Cambridge, Mass, 1970.
4. D. M. Ruthven, *Principles of Adsorption and Adsorption Processes*, J. Wiley and Sons, New York, 1984.
5. E. A. Mason and A. P. Malinauskas, *Gas Transport in Porous Media*: *The Dusty-gas Model*, Elsevier, Amsterdam, 1983.
6. M. M. Dubinin, *Zh. Fiz. Khim.*, 1960, **34**, 959 [*J. Phys. Chem. USSR*, 1960, **34** (Engl. Transl.)].
7. S. J. Gregg and K. G. W. Sing, *Adsorption, Surface Area and Porosity*, Academic Press, London, 1982.
8. Yu. K. Tovbin and E. V. Votyakov, *Izv. Akad. Nauk*, *Ser. Khim.*, 2001, 48 [*Russ. Chem. Bull*, *Int. Ed.*, 2001, **50**, 50].
9. Yu. K. Tovbin, *IX Mezhdunar. konf. po teoreticheskim voprosam adsorbtsii i adsorbtsionnoi khromatografii* [*Proc. Int. Conf. on the Theoretical Problems of Adsorption and Adsorption Chromatography*], Institute of Physical Chemistry, Russian Academy of Sciences, Moscow, 2001, 11 (in Russian).
10. S. F. Borisov, N. F. Balakhonov, and V. A. Gubanov, *Vzaimodeistviya gazov s poverkhnost'yu tverdogo tela* [*Interaction of Gases with a Solid Surface*], Nauka, Moscow, 1988, 200 pp. (in Russian).
11. B. D. Todd and D. J. Evans, *J. Chem. Phys.*, 1995, **103**, 9804.
12. J. M. D. MacElroy, *J. Chem. Phys.*, 1994, **101**, 5274.
13. E. Akhmatskaya, B. D. Todd, P. J. Davis, D. J. Evans, K. E. Gubbins, and L. A. Pozhar, *J. Chem. Phys.*, 1997, **106**, 4684.
14. *Adsorbtsiya v Mikroporakh* [*Adsorption in Micropores*], Eds. M. M. Dubinin and V. V. Serpinskii, Nauka, Moscow, 1983, 114 (in Russian).
15. R. Sh. Vartapetyan, A. M. Voloshchuk, and I. Kerger, *VIII Mezhdunar. konf. "Teoriya i praktika adsorbtsionnykh protsessov"* [*Proc. Int. Conf. on the Theory and Practice of Adsorption Processes*], Institute of Physical Chemistry, Russian Academy of Sciences, Moscow, 1997, 63 (in Russian).
16. B. D. Todd, P. J. Daivis, and D. J. Evans, *Phys. Rev.*, *E*, 1995, **51**, 4362.
17. K. P. Travis and D. J. Evans, *Phys. Rev.*, *E*, 1996, **55**, 1566.
18. K. P. Travis, B. D. Todd, and D. J. Evans, *Physica A*, 1997, **240**, 315.
19. M. M. Mansour, F. Baras, and A. L. Garsia, *Physica A*, 1997, **240**, 255.
20. J. O. Hirschfelder, C. F. Curtiss, and R. B. Bird, *Molecular Theory of Gases and Liquids*, Wiley, New York, 1954.
21. J. H. H. Ferziger and H. G. Kaper, *Mathematical Theory of Transport Processes in Gases*, North-Holland Publ. Comp., Amstredam—London, 1972.
22. C. A. Croxton, *Liquid State Physics — A Statistical Mechanical Introduction*, Cambridge Univer. Press, Cambridge, 1974.
23. Yu. K. Tovbin, *Zh. Fiz. Khim.*, 1998, **72**, 1446 [*Russ. J. Phys. Chem.*, 1998, **72**, No. 12 (Engl. Transl.)].
24. Yu. K. Tovbin, *Zh. Fiz. Khim.*, 2002, **76**, 76 [*Russ. J. Phys. Chem.*, 2002, **76**, No. 1 (Engl. Transl.)].
25. Yu. K. Tovbin, *Khim. Fiz.*, 2002, **21**, 83 [*Chem. Phys. Reports*, 2002, **21**, No. 1 (Engl. Transl.)].
26. R. B. Bird, W. E. Stewart, and E. N. Lightfoot, *Transport Phenomena*, J. Wiley and Sons, Inc., New York—London, 1965.
27. V. A. Rabinovich, A. A. Vasserman, V. I. Nedostup, and L. S. Veksler, *Teplofizicheskie svoistva neona*, *argona*, *kriptona i ksenona* [*Thermal Properties of Neon, Argon, Krypton, and Xenon*], Izd. standartov, Moscow, 1976 (in Russian).
28. M. A. Anisimov, V. A. Rabinovich, and V. V. Sychev, *Termodinamika kriticheskogo sostoyaniya* [*Critical State Thermodynamics*], Energoatomizdat, Moscow, 1990, 190 pp. (in Russian).
29. *Statistical Mechanics. Principles and Selected Applications*, McGraw-Hill Book Comp. Inc., New York, 1956.
30. Yu. K. Tovbin, *Theory of Physicochemical Processes at the Gas—Solid Interface*, CRC Press Inc., Boca Raton, Fr., 1991.
31. E. V. Votyakov, Yu. K. Tovbin, J. M. D. MacElroy, and A. Roche, *Langmuir*, 1999, **15**, 5713.
32. A. M. Vishnyakov, E. M. Piotrovskaya, E. N. Brodskaya, E. V. Votyakov, and Yu. K. Tovbin, *Zh. Fiz. Khim.*, 2000, **74**, 501 [*Russ. J. Phys. Chem.*, 2000, **74**, No. 3 (Engl. Transl.)].
33. Yu. K. Tovbin, and N. F. Vasyutkin, *Zh. Fiz. Khim.*, 2002, **76**, 319 [*Russ. J. Phys. Chem.*, 2002, **76**, No. 2 (Engl. Transl.)].
34. Yu. K. Tovbin, *Zh. Fiz. Khim.*, 1995, **69**, 118 [*Russ. J. Phys. Chem.*, 1995, **69**, No. 1 (Engl. Transl.)].
35. E. A. Moelwyn-Hughes, *Physical Chemistry*, Pergamon Press, London—New York—Paris, 1961.
36. Yu. K. Tovbin and E. V. Votyakov, *Langmuir*, 1993, **9**, 2652.
37. V. A. Pindyurin, S. Yu. Surovtsev, and Yu. K. Tovbin, *Zh. Fiz. Khim.*, 1986, **60**, 945 [*Russ. J. Phys. Chem.*, 1986, **60**, No. 4 (Engl. Transl.)].
38. Yu. K. Tovbin, *Dokl. Akad. Nauk SSSR*, 1990, **312**, 1423 [*Dokl. Chem.*, 1990 (Engl. Transl.)].
39. Yu. K. Tovbin, *Progress in Surface Science*, 1990, **34**, 1.
40. Yu. K. Tovbin and E. V. Votyakov, *Izv. Akad. Nauk*, *Ser. Khim.*, 2000, 605 [*Russ. Chem. Bull*, *Int. Ed.*, 2000, **49**, 609].
41. B. V. Egorov, V. N. Komarov, Yu. E. Markachev, and Yu. K. Tovbin, *Zh. Fiz. Khim.*, 2000, **74**, 882 [*Russ. J. Phys. Chem.*, 2000, **74**, No. 5 (Engl. Transl.)].
42. Yu. K. Tovbin and V. N. Komarov, *Zh. Fiz. Khim.*, 2001, **75**, 579 [*Russ. J. Phys. Chem.*, 2001, **75**, No. 3 (Engl. Transl.)].
43. Yu. K. Tovbin, *Zh. Fiz. Khim.*, 1988, **72**, 865 [*Russ. J. Phys. Chem.*, 1998, **72**, No. 5 (Engl. Transl.)].
44. W. A. Steele, *The Interactions of Gases with Solid Surfaces*, Pergamon, New York, 1974.
45. S. Sokolowski and J. Fischer, *Mol. Phys.*, 1990, **71**, 393.
46. Yu. K. Tovbin, M. M. Senyavin, and L. K. Zhidkova, *Zh. Fiz. Khim.*, 1999, **73**, 301 [*Russ. J. Phys. Chem.*, 1999, **73**, No. 2 (Engl. Transl.)].
47. J. A. Barker and D. Henderson, *Rev. Mod. Phys.*, 1976, **48**, 587.
48. O. Yu. Batalin, Yu. K. Tovbin, and V. K. Fedyanin, *Zh. Fiz. Khim.*, 1980, **53**, 3020 [*Russ. J. Phys. Chem.*, 1980, **53**, No. 12 (Engl. Transl.)].

Received December 6, 2001;
in revised form March 29, 2002